Quantum Thermopower of Metallic Atomic-Size Contacts at Room Temperature

Charalambos Evangeli,[†] Manuel Matt,[‡] Laura Rincón-García,[†,§] Fabian Pauly,[‡] Peter Nielaba,[‡] Gabino Rubio-Bollinger,[†,‖] Juan Carlos Cuevas,*[⊥] and Nicolás Agraït*[†,§,‖]

[†]Departamento de Física de la Materia Condensada and Condensed Matter Physics Center (IFIMAC), Universidad Autónoma de Madrid, E-28049 Madrid, Spain

[‡]Department of Physics, University of Konstanz, D-78457 Konstanz, Germany

[§]Instituto Madrileño de Estudios Avanzados en Nanociencia IMDEA-Nanociencia, E-28049 Madrid, Spain

[‖]Instituto Universitario de Ciencia de Materiales "Nicolás Cabrera", Universidad Autónoma de Madrid, E-28049 Madrid, Spain

[⊥]Departamento de Física Teórica de la Materia Condensada and Condensed Matter Physics Center (IFIMAC), Universidad Autónoma de Madrid, E-28049 Madrid, Spain

ⓢ Supporting Information

ABSTRACT: We report conductance and thermopower measurements of metallic atomic-size contacts, namely gold and platinum, using a scanning tunneling microscope (STM) at room temperature. We find that few-atom gold contacts have an average negative thermopower, whereas platinum contacts present a positive thermopower, showing that for both metals, the sign of the thermopower in the nanoscale differs from that of bulk wires. We also find that the magnitude of the thermopower exhibits minima at the maxima of the conductance histogram in the case of gold nanocontacts while for platinum it presents large fluctuations. Tight-binding calculations and

Green's function techniques, together with molecular dynamics simulations, show that these observations can be understood in the context of the Landauer−Büttiker picture of coherent transport in atomic-scale wires. In particular, we show that the differences in the thermopower between these two metals are due to the fact that the elastic transport is dominated by the 6s orbitals in the case of gold and by the 5d orbitals in the case of platinum.

KEYWORDS: Quantum thermopower, quantum conductance, atomic-size metallic contacts, Landauer approach, molecular dynamics simulations
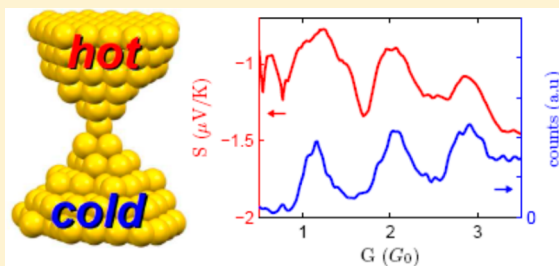
Thermoelectric devices hold the promise for helping to solve key problems related to energy conversion and refrigeration.[1] The discovery that nanostructured materials may enhance their efficiency[2] underlines the need to understand the mechanisms that govern thermoelectricity at the nanoscale. Although notable progress has been made in this respect,[3−5] there remain basic open problems. Thus, for instance, it is still unclear what determines the thermoelectricity in a metallic atomic-size contact,[6] a system that has become the test bed for nanoelectronics and mesoscopic physics.[7] Here we report room-temperature thermopower measurements of gold and platinum atomic-size contacts that show that even its sign differs from that of bulk wires. We find that gold few-atom contacts exhibit a negative thermopower whose magnitude presents minima at the maxima of the conductance histogram, whereas platinum contacts have an average positive thermopower with large fluctuations. We show that these observations can be understood within a picture of coherent electron transport and explain the differences between metals in terms of their distinct electronic structure. Our results illustrate that

thermoelectricity at the nanoscale differs substantially from the macroscopic limit.

If a temperature difference ΔT is applied across a metallic junction, an electric potential difference ΔV appears in response (Seebeck effect). This effect is quantified by the thermopower or Seebeck coefficient that is defined as $S = -\Delta V/\Delta T$. In macroscopic metallic wires, the thermopower has two contributions due to both electron diffusion and phonon drag.[8] The phonon drag contribution plays a very important role at low temperatures (lower than the Debye temperature). However, the thermopower at room temperature in metals is dominated by the diffusion contribution,[8] which is qualitatively understood since the pioneering work of Sir N. F. Mott.[9] The sign and the magnitude of the room temperature thermopower in metals depend on the energy dependence of the conductivity around the Fermi energy, which in turn depends on the inelastic relaxation time and the effective mass.[8,9] Thus, for
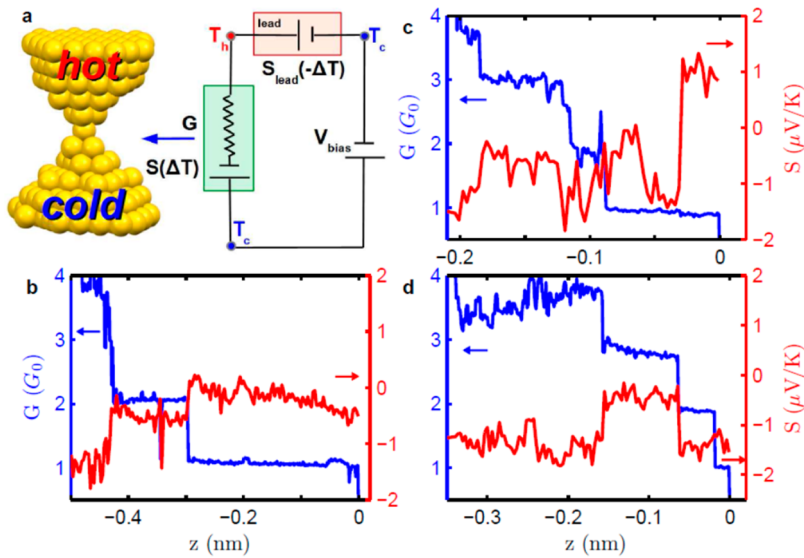
Figure 1. Simultaneous measurement of the conductance and thermopower of metallic atomic-size contacts. (a) Schematic representation of the setup used to measure simultaneously conductance and thermopower in metallic atomic-size contacts. The tip is heated to a temperature T_h while the substrate is kept at room temperature T_c. A temperature gradient $\Delta T = T_h - T_c$ is established across the junction and along the tip-connecting lead. (b−d) Three characteristic examples of the conductance (blue curves) and thermopower (red curves) in the last stages of the breaking of an Au wire at room temperature. Both conductance and thermopower are very sensitive to atomic rearrangements at the junction. In some cases, an atomic rearrangement that produces just a small change in the conductance results in a huge change in the thermopower, as illustrated in panel c.

instance, the relatively large magnitude and negative sign of the thermopower of transition metals (like Ni, Pd, or Pt) is attributed to the increasing relaxation time with energy due to their characteristic density of states. This is clearly at variance with noble metals (Cu, Ag, and Au), which exhibit a smaller and positive thermopower.[9] This picture is valid only in the case of bulk metals and, as we shall show below, a different picture emerges at the nanoscale due to quantum effects.

The advent of experimental techniques like the scanning tunneling microscope (STM) and the mechanically controllable break junctions (MCBJs) has allowed investigating the transport properties of metallic atomic-size contacts.[7] These atomic wires have turned out to be ideal systems where quantum theories of charge and energy transport have been thoroughly tested.[7] However, thermoelectricity in these contacts has received little attention so far due to experimental challenges. The first measurements of the thermopower of an atomic-size contact were reported using gold MCBJs at 12 K.[6] The thermopower was found to be different in each experimental realization and to have a very small average value, while its fluctuations were explained in terms of interference effects due to the presence of impurities near the contact region. However, in very recent experiments[10] the room-temperature thermopower of gold atomic-size contacts has been shown to have a nonzero average value and to exhibit oscillations as a function of the contact size that were attributed to quantum confinement. This apparent contradiction has renewed the interest in the basic question of how the thermopower of atomic-scale metallic wires depends on the material, the size of the contacts, and their geometry.

To address these questions, we have studied the thermo-power of Au−Au and Pt−Pt atomic-size contacts, using a modified STM setup.[11] The gold (single crystal, 99.999% purity) and platinum (99.99% purity) surfaces are flamed annealed. In addition, Pt is chemically etched with aqua regia (HNO$_3$/HCl 1:3). We use mechanically cut Au and Pt tips and the contacts are formed by controlled indentation of the

substrate with the STM tip and subsequent separation.[12,13] The STM tip is heated with a resistive element while keeping the substrate at room temperature, and a voltage bias V_{bias} is applied to the substrate. We measure with temperature differences between the tip and the substrate of 20 and 40 K. This temperature difference ΔT gives rise to a thermovoltage V_{th}, which consists of a contribution from the contact $S\Delta T$ and a contribution from the tip-connecting lead $S_{lead}(-\Delta T)$, where S and S_{lead} are the thermopower of the contact and the lead, respectively. The current between the tip and substrate is given by

$$I = G(V_{bias} - V_{th}) = G(V_{bias} + S_{lead}\Delta T - S\Delta T) \qquad (1)$$

where G is the conductance of the contact (see Figure 1a). Taking into account that for $V_{bias} = V_{th}$ the current vanishes, by measuring an $I-V$ curve we can obtain simultaneously the thermopower and the conductance: the zero crossing yields V_{th} (and hence S) and the slope gives G (see Supporting Information for more details).

In Figure 1b−d, we show some characteristic examples of the simultaneous measurements of the conductance G and thermopower S in the last stages of the breaking of Au wires. As it is well-known for Au contacts,[14] the conductance decreases in a steplike manner due to atomic rearrangements in the contact[15,16] with a tendency to exhibit plateaus close to multiples of the conductance quantum, $G_0 = 2e^2/h$, where e is the absolute value of the electron charge and h is the Planck constant. The thermopower also presents plateaus separated by abrupt variations in response to atomic rearrangements but evolves in a more complicated fashion exhibiting predominantly negative values but also positive ones (see Figure 1b−d). In particular, we observe that in the quantized conductance plateaus, the thermopower tends to be partially suppressed. This is particularly clear for junctions with $G \approx G_0$, which correspond to single-atom contacts or short atomic chains[17] (see Figure 1b).

To establish the characteristic behavior of the thermopower we have carried out a systematic statistical analysis collecting the data of a few hundreds of contact breakings. As we show in the density plot of Figure 2a, starting from very large contacts
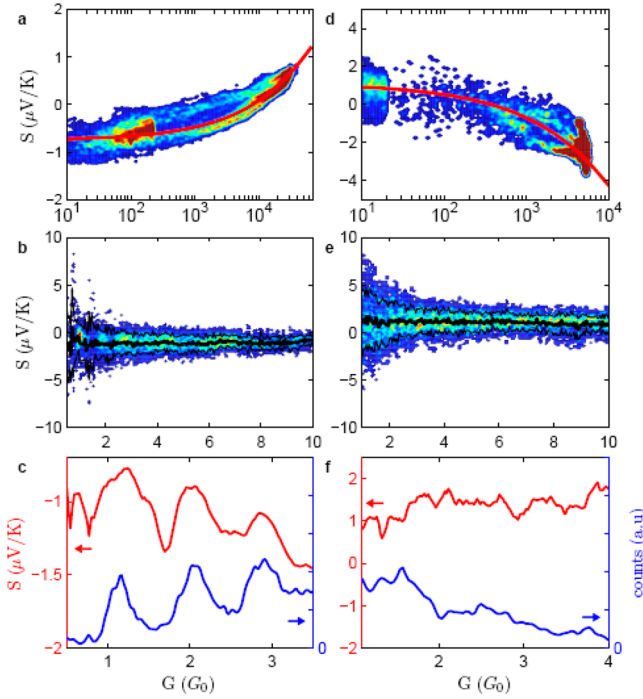

Figure 2. Thermopower of Au and Pt atomic-size contacts. (a,d) Density plots of the thermopower versus conductance for very large contacts (up to $10^4-10^5 G_0$) of 134 breakings of Au (a) and 263 of Pt contacts (d). Red thick lines show the fit that describes the transition between atomic contacts and bulk-like wires. The values used in the fit are the following: for Au, $S_S = -0.75$ μV/K and $S_M = 1.94$ μV/K; for Pt, $S_S = +1.1$ μV/K and $S_M = -5.3$ μV/K. (b,e) Thermopower density plots as a function of the conductance for small contacts up to $10 G_0$ of 674 and 385 breakings of Au (b) and Pt (e) contacts, respectively. Black thick lines show the average thermopower value and the black thin lines the region around the average value within the standard deviation. The mean value of thermopower is negative for Au and positive for Pt. The sign of the mean thermopower changes from negative (positive) for small atomic contacts of Au (Pt) to positive (negative) for large contacts. (c,f) Conductance histogram (blue) and average thermopower (red) for few atom contacts ($G < 4G_0$) of 909 breaking curves on Au (c) and 216 breaking curves on Pt (f). The magnitude of the thermopower of Au exhibits minima coinciding with the maxima of the conductance histogram, while for Pt there is not any pronounced feature. See Supporting Information Figure S4 for the corresponding density plots.

with $G > 10^4 G_0$, where $S \approx +1$ μV/K in fair agreement with bulk measurements,[18] we observe a crossover to negative values as the contact size is reduced. Focusing on few-atom contacts with $G < 10G_0$, see Figure 2b, we find that the thermopower fluctuates from contact to contact, but its average value is negative independently of the conductance. Moreover, for the smallest contacts ($G < 4G_0$), the thermopower magnitude exhibits minima coinciding with the maxima of the conductance histogram (see Figure 2c), which are close to multiples of G_0.

Turning now to the results for Pt contacts, we observe that the thermopower changes from large negative values of $S \approx +1$ μV/K, close to the known bulk result,[19] to positive values as the contact size diminishes (see Figure 2d). As one can see in

Figure 2e, Pt few-atom contacts exhibit an average positive thermopower with fluctuations that are several times larger than for Au. Finally, for the smallest contacts there is not a simple correlation between the thermopower and the conductance (see Figure 2f).

To elucidate the origin of the behavior of the thermopower of atomic-size contacts we computed the transport properties of these nanowires within the Landauer–Büttiker approach to coherent transport.[20] In this approach, the conductance and the thermopower are expressed in terms of the energy-dependent transmission function $\tau(E)$ as

$$G = G_0 K_0(T) \quad \text{and} \quad S = -\frac{K_1(T)}{eTK_0(T)} \quad (2)$$

with $K_n(T) = \int dE (E - E_F)^n \tau(E)[-\partial_E f(E,T)]$. Here, E_F is the Fermi energy and $f(E,T)$ is the Fermi function. At low temperatures, these expressions reduce to $G = G_0 \tau(E_F)$ and $S = -[(\pi^2 k_B^2 T/3e)][\partial_E \ln \tau(E)]_{E=E_F}$, where k_B is the Boltzmann constant. The total transmission can be resolved into the transmission coefficients of the conduction eigenchannels, τ_i, as $\tau(E) = \sum_i \tau_i (E)$. Thus, within this approach the technical task is the calculation of the energy dependence of the transmission. For this purpose, we first carried out classical molecular dynamics (MD) simulations to describe the formation of the atomic contacts. These simulations were performed with the code LAMMPS[21] within the embedded atom method.[22] Then, once the geometries of the atomic wires were determined, we computed the transmission coefficients by combining a tight-binding model[23] for the electronic structure and Green's function techniques[24−26] (see Supporting Information).

We simulated 100 stretching events for Au and Pt wires at 300 K oriented in the ⟨100⟩ direction to obtain a reliable statistics. Our main results for the thermopower and the conductance of Au and Pt contacts are summarized in Figure 3. Let us remark that while the low-temperature approximation for the conductance gives excellent results (with 1% errors), we found it necessary to employ the full formula of eq 2 to get accurate results for the thermopower. As one can see in Figure 3a,d, the thermopower changes from realization to realization with a negative average value for Au and a positive one for Pt, irrespective of the conductance value. Moreover, for Au contacts the magnitude of the thermopower exhibits minima correlated with the conductance maxima (Figure 3b) and in particular it is largely suppressed close to $1G_0$. The analysis of the transmission coefficients (see Figure 3c) shows that this suppression is due to the fact that the transport is dominated by a single fully open conduction channel due to the Au 6s orbitals.[27] Thus, the transmission reaches a maximum at the Fermi energy, which leads to a very small thermopower value at $1G_0$. Similarly, the other minima in the thermopower magnitude are due to the saturation of the transmission of other channels when the conductance is a multiple of G_0 In the case of Pt, there is no noticeable structure in the thermopower related to the main peak in the conductance histogram (∼$1.9G_0$, see Figure 3e) and in general the fluctuations are several times larger than in Au contacts. We attribute these features to the fact that the transport in Pt contacts is dominated by the 5d orbitals.[24] This implies that several partially open channels contribute to the transport even in single-atom contacts, see Figure 3f. Thus, the transmission does not reach an extremum at the Fermi energy and the thermopower is not suppressed. Moreover, the d orbitals are
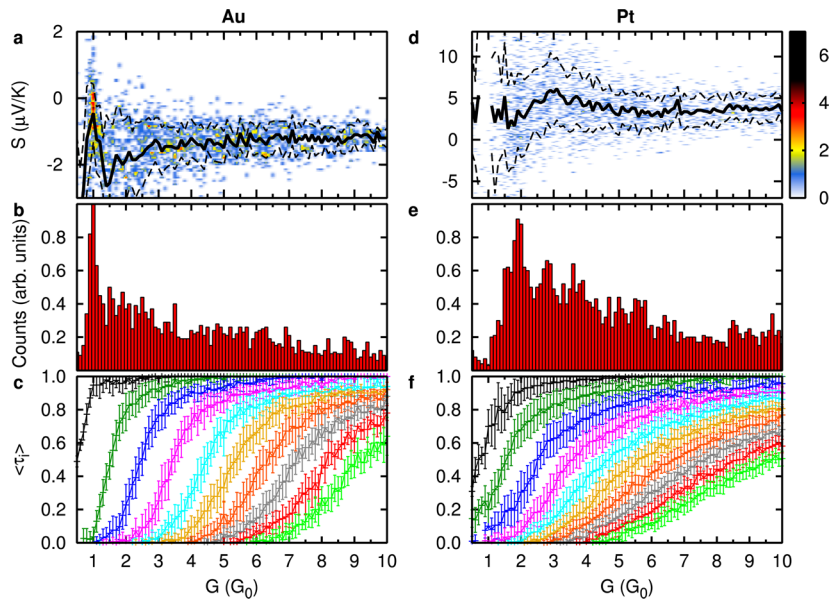
Figure 3. Computed thermopower and conductance. (a) Density plot of the thermopower as a function of the conductance computed from 100 simulations of the stretching of Au contacts at room temperature. The solid black line indicates the average value, while the dashed lines delimit the region around the average value within the standard deviation. Notice that the average value of S is negative. (b) The corresponding computed conductance histogram for Au contacts. The most salient feature is the appearance of a peak close to $1G_0$. (c) The 10 largest transmission coefficients as a function of the conductance. The lines correspond to the average values and the bars to the standard deviations. Notice that the region close to $1G_0$ is dominated by a single fully open channel. (d–f) The same as in panels a–c but for Pt. Notice that the average thermopower is positive. The conductance histogram exhibits a peak at around $1.9G_0$, which corresponds to single-atom contacts and short atomic chains. This conductance region is dominated on average by four conduction channels.
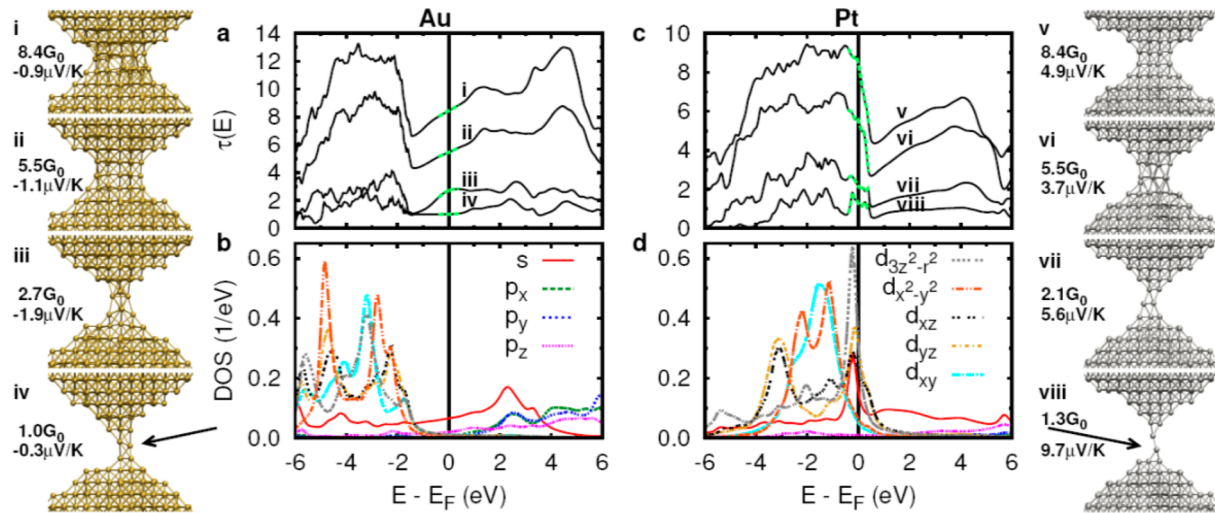

Figure 4. Origin of the sign of the thermopower. (a) Total transmission as a function of energy for the four Au contacts shown in the left column (i–iv), which correspond to different stages of the breaking of the same wire. The dashed green lines indicate the relevant energy used to compute the thermopower according to eq 2. Notice that the slope around the Fermi energy is positive, which leads to a negative thermopower. The values of the conductance and thermopower of those contacts are indicated next to the geometries. (b) Local density of states (DOS) as a function of energy projected onto the different atomic orbitals of the atom indicated with an arrow in the lower geometry. The legend is split into panels b and d. Here, z corresponds to the direction of the contact axis (or transport direction). Notice that the DOS is dominated by the s and p_z orbitals for which it exhibits a positive slope around the Fermi energy. (c,d) The same as in panels a and b for the Pt geometries shown in the right column (v–viii). Notice that in this case the transmission tends to exhibit a negative slope around the Fermi energy, which leads to a positive thermopower, while the local DOS is dominated by the 5d orbitals for which it decreases with increasing energy.

anisotropic and thus much more sensitive to local disorder than the s orbitals, which leads to larger fluctuations in the thermopower for Pt.[25] Overall, these results are in very good qualitative agreement with our experimental findings.

Let us now shed some more light on the origin of the sign of the thermopower. According to eq 2, this sign is determined by the electron–hole asymmetry in the transmission function. In Figure 4a,c, we show the total transmission as a function of energy for Au and Pt few-atom contacts obtained from the same stretching simulation. Notice that while the slope around the Fermi energy, E_F, is typically positive for the Au contacts, leading to a negative thermopower, it is mainly negative in the

case of Pt, which results in a positive thermopower. This different behavior can be traced back to the different electronic structure of these two metals. In the case of Au, E_F lies on a region dominated by the 6s orbitals with smaller contributions from the 6p bands. The density of states (DOS) for these orbitals, which are responsible for the transport, tends to slightly increase with energy. This is illustrated in Figure 4b where we show the local DOS projected onto the different orbitals of a central atom in a two-atom contact. On the contrary, for Pt, E_F lies close to the edge of the 5d bands, a region where the transmission typically diminishes with increasing energy. This reflects in turn the typical behavior of the local DOS, as we show in Figure 4d for a single-atom contact.

Let us now compare with previous results. For Au, our results are in qualitative agreement with those recently reported in ref 10, while the interpretation is clearly at variance. To explain their results, the authors of ref 10 invoked simple free-electron models meant to describe ballistic quantum point contacts.[28−30] However, these models only predict a negative sign for the thermopower and they are thus unable to explain the appearance of positive values in some Au contacts or the typical behavior of the Pt contacts. This shows that our results cannot be simply explained in terms of quantum confinement. On the other hand, the claim in ref 6 that the thermopower of Au contacts vanishes on average is because those experiments were performed at a much lower temperature (12 K) and thus, the thermopower is expected to be around 30 times smaller than in our case.[25] Moreover, the role of the impurities advocated in that work to explain the behavior of the thermopower fluctuations is certainly important, but in our simulations the origin of thermopower fluctuations can be traced back to local disorder, underlining the importance of the detailed atomic arrangement at the contact. In contrast, the average behavior and in particular the characteristic sign of the thermopower is determined by the intrinsic electronic structure of the metal.

Comparing to our previous theoretical work[25] the technical approach is essentially identical. Main changes concern the number of atoms in the central wire (563 here as compared to 112 there) and the electronic and phononic temperatures of 300 K, as compared to 12 and 4.2 K in ref 25, respectively. Because of the lower temperatures, our theoretical results in ref 25 were indeed in agreement with those of ref 6. Upon close inspection, the statistically averaged thermopower of Au in Figure 4 of ref 25 is negative and shows a suppression at a conductance of $1G_0$, while for the Pt contacts in contrast it is indeed slightly positive. Let us point out that due to the smaller contact size in ref 25, only junctions with rather low conductance values up to $2-3G_0$ are not affected by the starting configurations in our MD simulations. The larger contacts used here allow us to discuss the thermopower reliably up to much higher conductances, reproducing the oscillations and the nonzero offset of the thermopower.

Let us now consider in more detail the variation of the thermopower from the bulk value to the atomic contact value. In Figure 2a,d, the thermopower is plotted as a function of the conductance of the contact, which is related to the contact radius, a. For radii smaller than the inelastic electron mean free path l, the electron traverses the contact coherently (ballistically) and the conductance is given by Sharvin's expression:[7] $G_S = G_0(k_F a/2)^2$, where k_F is the Fermi wavenumber. For $a \gg l$, the electrons move through the

contact diffusively and Maxwell's expression for the spreading conductance must be used:[7] $G_M = 2a/\rho$, where ρ is the resistivity. The transition from the coherent (ballistic) regime to the diffusive regime may be described by a simple formula as $G = xG_S + (1 - x)G_M$, where x goes from a value of one for an atomic contact to zero for a contact larger than the electron mean free path. We may choose a simple form like $x = e^{-a/l}$. A similar formula should be valid for the variation of the thermopower with contact size becauyse, as discussed above, in this range of temperatures phonon drag effects are negligible in bulk and only electron diffusion needs to be considered. Thus, we write $S = xS_S + (1 - x)S_M$, where S_S is the thermopower in the atomic scale and S_M is the corresponding bulk value. Using l as a free parameter for the fit of the average thermopower, we obtain the red solid lines in Figure 2a,d. The best fit is obtained for values of l of 37 and 14 nm for Au and Pt, respectively, which are in good agreement with the inelastic mean free path obtained from the resistivity[31] (38 nm for Au and 8 nm for Pt). The fact that this simple analytical expression describes so well the transition between atomic contacts and bulk wires clearly suggests that this crossover is indeed determined by the ratio a/l and it originates from the change in the dominant transport mechanism.

In summary, we have shown that metallic contacts offer the unique possibility of investigating how thermoelectricity is continuously modified from bulklike devices all the way down to the atomic scale. Moreover, we have shown that the change in the dominant transport mechanism from incoherent transport in bulk samples to coherent one in atomic-scale wires leads to a qualitative modification of the thermopower, a very important lesson for the fields of thermoelectrics and nanoelectronics.

■ ASSOCIATED CONTENT

Ⓢ Supporting Information

Experimental technique; thermal circuit; thermovoltage calibration; density plots of few-atom contacts ($G < 4G_0$); simultaneous measurement of conductance and thermopower of Pt atomic-size contacts; and theoretical modeling: molecular dynamics simulations and transport calculations. This material is available free of charge via the Internet at http://pubs.acs.org.

■ AUTHOR INFORMATION

Corresponding Authors
*E-mail: (J.C.C.) juancarlos.cuevas@uam.es.
*E-mail: (N.A.) nicolas.agrait@uam.es.

Author Contributions
C.E. and L.R.-G. performed the experiments and M.M. carried out the MD simulations and the thermopower calculations. C.E. performed the calibration of the setup for the thermopower measurements. F.P., P.N., J.C.C., G.R.-B., and N.A. planned the project and advised the students. J.C.C. and N.A. wrote the manuscript with contributions from all the authors.

Notes
The authors declare no competing financial interest.

■ ACKNOWLEDGMENTS

■ REFERENCES

(1) Alam, H.; Ramakrishna, S. A review on the enhancement of figure of merit from bulk to nano-thermoelectric materials. *Nano Energy* **2013**, *2*, 190−212.

(2) Vineis, C. J.; Shakouri, A.; Majumdar, A.; Kanatzidis, M. G. Nanostructured thermoelectrics: Big efficiency gains from small features. *Adv. Mater.* **2010**, *22*, 3970−3980.

(3) Bulusu, A.; Walker, D. G. Review of electronic transport models for thermoelectric materials. *Superlattices Microstruct.* **2008**, *44*, 1−36.

(4) Pichanusakorn, P.; Bandaru, P. Nanostructured thermoelectrics. *Mater. Sci. Eng. R* **2010**, *67*, 19−63.

(5) Dubi, Y.; Di Ventra, M. Colloquium: Heat flow and thermoelectricity in atomic and molecular junctions. *Rev. Mod. Phys.* **2011**, *83*, 131−155.

(6) Ludoph, B.; van Ruitenbeek, J. M. Thermopower of atomic-size metallic contacts. *Phys. Rev. B* **1999**, *59*, 12290−12293.

(7) Agraït, N.; Yeyati, A. L.; van Ruitenbeek, J. M. Quantum properties of atomic-sized conductors. *Phys. Rep.* **2003**, *377*, 81−279.

(8) Blatt, F. J.; Schroeder, P. A.; Foiles, C. L.; Greig, D. *Thermoelectric Power of Metals*; Plenum Press: New York, 1976.

(9) Mott, N. F.; Jones, H. *The Theory of the Properties of Metals and Alloys.*; Oxford University Press: London, 1936.

(10) Tsutsui, M.; Morikawa, T.; Arima, A.; Taniguchi, M. Thermoelectricity in atomic-sized junctions at room temperatures. *Sci. Rep.* **2013**, *3*, 3326.

(11) Evangeli, C.; Gillemot, K.; Leary, E.; González, M. T.; Rubio-Bollinger, G.; Lambert, C. J.; Agraït, N. Engineering the Thermopower of C_{60} Molecular Junctions. *Nano Lett.* **2013**, *13*, 2141−2145.

(12) Agraït, N.; Rubio, G.; Vieira, S. Plastic Deformation of Nanometer-Scale Gold Connective Necks. *Phys. Rev. Lett.* **1996**, *74*, 3995−3998.

(13) Untiedt, C.; Rubio, G.; Vieira, S.; Agraït, N. Fabrication and characterization of metallic nanowires. *Phys. Rev. B* **1997**, *56*, 2154−2160.

(14) Agraït, N.; Rodrigo, J. G.; Vieira, S. Conductance steps and quantization in atomic-size contacts. *Phys. Rev. B* **1993**, *47*, 12345−12348.

(15) Rubio, G.; Agraït, N.; Vieira, S. Atomic-sized metallic contacts: mechanical properties and electronic transport. *Phys. Rev. Lett.* **1996**, *76*, 2302−2305.

(16) Rubio-Bollinger, G.; Bahn, S. R.; Agraït, N.; Jacobsen, K. W.; Vieira, S. Mechanical properties and formation mechanisms of a wire of single gold atoms. *Phys. Rev. Lett.* **2001**, *87*, 026101.

(17) Yanson, A. I.; Rubio Bollinger, G.; van den Brom, H. E.; Agraït, N.; van Ruitenbeek, J. M. Formation and manipulation of a metallic wire of single gold atoms. *Nature* **1998**, *395*, 783−785.

(18) Cusak, N.; Kendall, P. The absolute scale of thermoelectric power at high temperature. *Proc. Phys. Soc.* **1958**, *72*, 898−901.

(19) Moore, J. P.; Graves, R. S. Absolute Seebeck coefficient of platinum from 80 to 340 K and the thermal and electrical conductivities of lead from 80 to 400 K. *J. Appl. Phys.* **1973**, *44*, 1174−11178.

(20) Cuevas, J. C.; Scheer, E. *Molecular Electronics: An Introduction to Theory and Experiment*; World Scientific: Singapore, 2010.

(21) Plimpton, S. Fast Parallel Algorithms for Short-Range Molecular Dynamics. *J. Comp. Phys.* **1995**, *117*, 1−19.

(22) Sheng, H. W.; Kramer, M. J.; Cadien, A.; Fujita, T.; Chen, M. W. Highly-optimized EAM potentials for 14 fcc metals. *Phys. Rev. B* **2011**, *83*, 134118.

(23) Mehl, M. J.; Papaconstantopoulos, D. A. *Computational Materials Science*; Fong,C., Ed.; World Scientific: Singapore, 1998.

(24) Pauly, F.; Dreher, M.; Viljas, J. K.; Häfner, M.; Cuevas, J. C.; Nielaba, P. Theoretical analysis of the conductance histograms and structural properties of Ag, Pt and Ni nanocontacts. *Phys. Rev. B* **2006**, *74*, 235106.

(25) Pauly, F.; Viljas, J. K.; Burkle, M.; Dreher, M.; Nielaba, P.; Cuevas, J. C. Molecular dynamics study of the thermopower of Ag, Au and Pt nanocontacts. *Phys. Rev. B* **2011**, *84*, 195420.

(26) Schirm, C.; Matt, M.; Pauly, F.; Cuevas, J. C.; Nielaba, P.; Scheer, E. A current-driven single-atom memory device. *Nat. Nanotechnol.* **2013**, *8*, 645−658.

(27) Scheer, E.; Agraït, N.; Cuevas, J. C.; Yeyati, A. L.; Ludoph, B.; Martín-Rodero, A.; Bollinger, G. R.; van Ruitenbeek, J. M.; Urbina, C. The signature of chemical valence in the electrical conduction through a single-atom contact. *Nature* **1998**, *394*, 154−157.

(28) Streda, P. Quantised thermopower of a channel in the ballistic regime. *J. Phys.: Condens. Matter* **1989**, *1*, 1025−1027.

(29) van Houten, H.; Molenkamp, L. W.; Beenakker, C. W. J.; Foxon, C. T. Thermoelectric properties of quantum point contacts. *Semicond. Sci. Technol.* **1992**, *7*, B215−B221.

(30) Bogachek, E. N.; Scherbakov, A. G.; Landman, U. Thermopower of quantum nanowires in a magnetic field. *Phys. Rev. B* **1996**, *54*, R11094−R11097.

(31) Ashcroft, N. W.; Mermin, N. D. *Solid State Physics*; Saunders: Philadelphia, PA, 1976.